Cholesterol reduction impairs exocytosis of synaptic vesicles

Anna Linetti[1], Alessandra Fratangeli[1], Elena Taverna[1,*], Pamela Valnegri[1], Maura Francolini[1], Valentina Cappello[1], Michela Matteoli[1,2], Maria Passafaro[1,3] and Patrizia Rosa[1,‡]

[1]CNR-Institute of Neuroscience, Department of Medical Pharmacology, University of Milan, 20129 Milan, Italy
[2]IRCCS Fondazione Don Gnocchi, 20149, Milan, Italy
[3]DTI, Dulbecco Telethon Institute, 20129, Milan, Italy

*Present address: Max-Planck-Institute of Molecular Cell Biology and Genetics, 01307 Dresden, Germany
‡Author for correspondence (p.rosa@in.cnr.it)

Accepted 20 November 2009
Journal of Cell Science 123, 595-605

doi:10.1242/jcs.060681

Summary

Cholesterol and sphingolipids are abundant in neuronal membranes, where they help the organisation of the membrane microdomains involved in major roles such as axonal and dendritic growth, and synapse and spine stability. The aim of this study was to analyse their roles in presynaptic physiology. We first confirmed the presence of proteins of the exocytic machinery (SNARES and $Ca_v2.1$ channels) in the lipid microdomains of cultured neurons, and then incubated the neurons with fumonisin B (an inhibitor of sphingolipid synthesis), or with mevastatin or zaragozic acid (two compounds that affect the synthesis of cholesterol by inhibiting HMG-CoA reductase or squalene synthase). The results demonstrate that fumonisin B and zaragozic acid efficiently decrease sphingolipid and cholesterol levels without greatly affecting the viability of neurons or the expression of synaptic proteins. Electron microscopy showed that the morphology and number of synaptic vesicles in the presynaptic boutons of cholesterol-depleted neurons were similar to those observed in control neurons. Zaragozic acid (but not fumonisin B) treatment impaired synaptic vesicle uptake of the lipophilic dye FM1-43 and an antibody directed against the luminal epitope of synaptotagmin-1, effects that depended on the reduction in cholesterol because they were reversed by cholesterol reloading. The time-lapse confocal imaging of neurons transfected with ecliptic SynaptopHluorin showed that cholesterol depletion affects the post-depolarisation increase in fluorescence intensity. Taken together, these findings show that reduced cholesterol levels impair synaptic vesicle exocytosis in cultured neurons.

Key words: Cholesterol, Regulated exocytosis, Sphingolipids, SNARE proteins, Synapses, Synaptic vesicles

Introduction

Cholesterol and sphingolipids can form dynamic platforms of different sizes and compositions in membranes (lipid microdomains or rafts) (Simons and Ikonen, 1997; Brown and London, 1998; Simons and Vaz, 2004; Pike, 2004; Pike, 2006; Mishra and Joshi, 2007). In neurons, cholesterol- and/or cholesterol-sphingolipid-based microdomains influence the function of various molecules, including neurotransmitters, growth factor receptors, ion channels, and cytoskeletal and adhesion molecules, and are therefore likely to modulate processes such as neurite outgrowth, receptor signalling, spine morphology and post-synaptic stability (Tsui-Pierchala et al., 2002; Hering et al., 2003; Golub and Caroni, 2005; Kamiguchi, 2006; Willmann et al., 2006; Allen et al., 2007). They can also recruit a number of presynaptic proteins, including soluble *N*-ethylmaleimide-sensitive factor attachment protein receptors (SNAREs) and the voltage-gated calcium channel $Ca_v2.1$ (also referred to as the P/Q-type channel) (Chamberlain et al., 2001; Lang et al., 2001; Jia et al., 2006; Taverna et al., 2004; Taverna et al., 2007). Finally, cholesterol is highly enriched in the membranes of synaptic vesicle, where it might be involved in vesicle biogenesis (Thiele et al., 2000; Takamori et al., 2006) and/or membrane fusion, as indicated by membrane fusion of sea urchin cortical vesicles and recent cell-free data relating to unilamellar vesicles containing SNARE proteins (Churchward et al., 2005; Churchward et al., 2008; Tong et al., 2009).

Lipid microenvironments therefore play an important role in the physiology and activity of presynapses, but there is little published information regarding living neurons, and no studies have yet tried to discriminate the functions of cholesterol-sphingolipid-based and cholesterol-based microdomains. Furthermore, what is known about the role of lipid microdomains in the function of synaptic vesicle fusion complexes has come from studies using the cholesterol-chelating agent methyl-β-cyclodestrin (MBCD) or statins (Chamberlain et al., 2001; Lang et al., 2001; Taverna et al., 2004; Zamir and Charlton, 2006; Wasser et al., 2007), and both approaches have their weaknesses. For example, a number of studies have reported that MBCD, used as a cholesterol-depletion agent, might have pleiotropic effects on the distribution of different membrane components and is capable of removing cholesterol from the liquid-ordered (lipid microdomains) and liquid-disordered phase (non-lipid microdomains) (Zidovetzki and Levitan, 2007), and it is still questionable whether the effects of statins are specifically assigned to cholesterol depletion (Schulz et al., 2004). By inhibiting the synthesis of mevalonate, statins reduce the levels of farnesyl diphosphate (Repko and Maltese, 1989), which is required for protein isoprenylation, a lipid modification that modulates the functioning of a number of signalling proteins, including the small GTP binding proteins of the Ras/Rho family (Pechlivanis and Kuhlmann, 2006) that play major roles in axonal growth, vesicular trafficking and synapse formation and stability (Fischer von Mollard et al., 1994; Jahn et al., 2003; Newey et al., 2005).

In order to investigate the role of cholesterol- and cholesterol-sphingolipid-rich microdomains in presynaptic physiology, we incubated hippocampal neurons after 14 days in vitro (DIV) with

fumonisin B1 (an inhibitor of dihydroceramide synthase), mevastatin (an inhibitor of mevalonate synthesis) or zaragozic acid, an inhibitor of squalene synthase (Bergstrom et al., 1993) that catalyses the first reaction of the mevalonate-isoprenoid pathway exclusively committed to cholesterol biosynthesis, and then investigated presynaptic activity by analysing synaptic vesicle cycling using FM1-43 and anti-synaptotagmin-1 antibody assays, and quantified the fluorescence intensity of ecliptic SynaptopHluorin (SypH) after depolarisation in control and cholesterol-depleted neurons (Betz and Bewick, 1992; Matteoli et al., 1992; Miesenböck et al., 1998).

Our results show that zaragozic acid, which greatly reduces cholesterol, also reduces the uptake of FM1-43 and anti-synaptotagmin-1 antibody, as well as the increase in SypH fluorescence intensity upon depolarisation, without affecting the number or size of synaptic vesicles, thus indicating that cholesterol plays an important role in neurotransmitter release.

Results

Lipid microdomains in presynaptic terminals of cultured hippocampal neurons

In order to verify whether cholesterol- and/or cholesterol-sphingolipid-based domains are involved in the organisation and physiology of presynapses, we used rat hippocampal neurons that had been cultured for at least 14 DIV because they are rich in synaptic contacts that have the morphological features of in situ presynapses (Matteoli et al., 2004).

We started by investigating whether in cultured neurons presynaptic proteins are also present in lipid microdomains, using a biochemical method to assess the presence of exocytic machinery in detergent-resistant membranes (DRMs) isolated from 21-26 DIV hippocampal neurons by means of extraction with 1% Triton X-100 and flotation on a sucrose-step gradient (Taverna et al., 2004). As shown in Fig. 1 (left panel), DRMs were recovered in fractions 3-5 of the gradients as assessed on the basis of their monosialotetrahexosylganglioside 1 (GM1) and flotillin flotation profiles. Soluble proteins were recovered in fractions 8-10 as has been previously demonstrated by the distribution of transferrin receptors (Taverna et al., 2004). In line with previous data (Chamberlain et al., 2001; Lang et al., 2001; Taverna et al., 2004), various amounts of exocytic machinery proteins such as syntaxin-1, SNAP-25, VAMP-2 (vesicle associated membrane protein 2, also referred to as synaptobrevin 2) and synaptotagmin-1 were recovered in fractions 3-5 (peaking in fraction 3), thus suggesting that they at least partially associate with lipid microdomains. In fully differentiated cultured neurons, $Ca_v2.1$ was mainly localised at the presynaptic boutons (as demonstrated by the colocalisation of the α1A channel subunit with presynaptic markers; supplementary material Fig. S1); in the flotation gradients, it was predominantly detected in DRMs (Fig. 1, left panel). The localisation of these proteins in DRMs is further supported by the flotation profile obtained after saponin treatment. As shown in Fig. 1 (right panel), all of the proteins were exclusively recovered in the soluble fraction (8-10) after saponin and Triton X-100 extraction from the neuronal cultures. Taken together, these data indicate that proteins of the exocytic machinery (SNAREs and $Ca_v2.1$) are associated with lipid microdomains in cultured hippocampal neurons.

We also used an immunofluorescent method to visualise lipid microdomains in neurons in order to distinguish the proteins associated with lipid or non-lipid microdomains on the basis of the operational definition of lipid microdomains as membrane regions

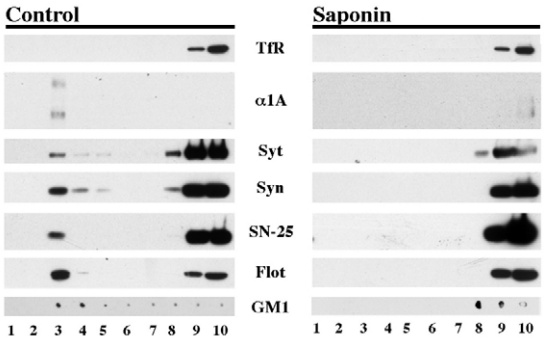

Fig. 1. Lipid microdomains in hippocampal neurons. The distribution of the transferrin receptor (TfR), the α1A subunit of $Ca_v2.1$ (α1A), synaptotagmin-1 (Syt), syntaxin-1 (Syn), SNAP-25 (SN-25), and flotillin (Flot) was analysed by means of western blotting of equal volumes of the gradient fractions (lanes 1-10) collected from continuous sucrose gradients of DIV 24 hippocampal neuron total membranes lysed in Triton X-100 (Control) or saponin and Triton X-100 (Saponin). The distribution of the GM1 marker was determined by means of labelling with peroxidase-conjugated cholera toxin. The figure shows representative blots of three independent experiments.

that are insoluble in cold anionic detergents (Simons and Ikonen, 1997; Brown and London, 1998; Hering et al., 2003). To test the efficacy of the method, we extracted 26 DIV hippocampal neurons in ice-cold Triton X-100 or saponin and Triton X-100 (see Materials and Methods) and, after treatment, fixed them and immunolabelled them with various markers. As expected, we found that the lipid microdomain-resident glycolipid GM1 was resistant to Triton X-100 extraction but completely solubilised after saponin pre-treatment, whereas transferrin receptor (a marker of detergent-soluble proteins) was fully solubilised by Triton X-100. By contrast, bassoon, a cytomatrix protein of the pre-synaptic active zones (Garner et al., 2000; Siksou et al., 2007), largely resisted extraction with both detergents (supplementary material Fig. S2 and Fig. 2).

In the light of these results, we next compared the staining of the α1A subunit of $Ca_v2.1$ and SNAP-25 with that of bassoon used to reveal neurons and presynaptic boutons even after saponin treatment. As shown in Fig. 2, the intensity of the immunostaining for α1A and SNAP-25 was reduced after Triton X-100 treatment but almost completely abolished after saponin preincubation.

Effects of cholesterol and sphingolipid-perturbing drugs on neurons and synaptic proteins

In order to test the role of cholesterol or sphingolipids in presynapses, we incubated hippocampal neurons with fumonisin B, zaragozic acid, or mevastastin and mevalonate (the latter was added to avoid completely inhibiting the synthesis of non-sterol compounds) (Ledesma et al., 1998), and analysed cholesterol and sphingolipid levels in control and treated cultures after 7 days.

Cholesterol levels were evaluated by means of a colorimetric assay or filipin labelling (Taverna et al., 2004; Simons et al., 1998). Filipin staining indicated that cholesterol levels in the mevastatin- and mevalonate-treated neurons were 20% lower than in controls (Fig. 3A; 78.64±2.87% of control; n=24 neurons from two experiments), and similar results were obtained with the colorimetric assay (not shown). Cholesterol synthesis was more efficiently inhibited by zaragozic acid, as indicated by the significant reduction in filipin fluorescence to ~50% (Fig. 3A, 50.06±2.13% of control;

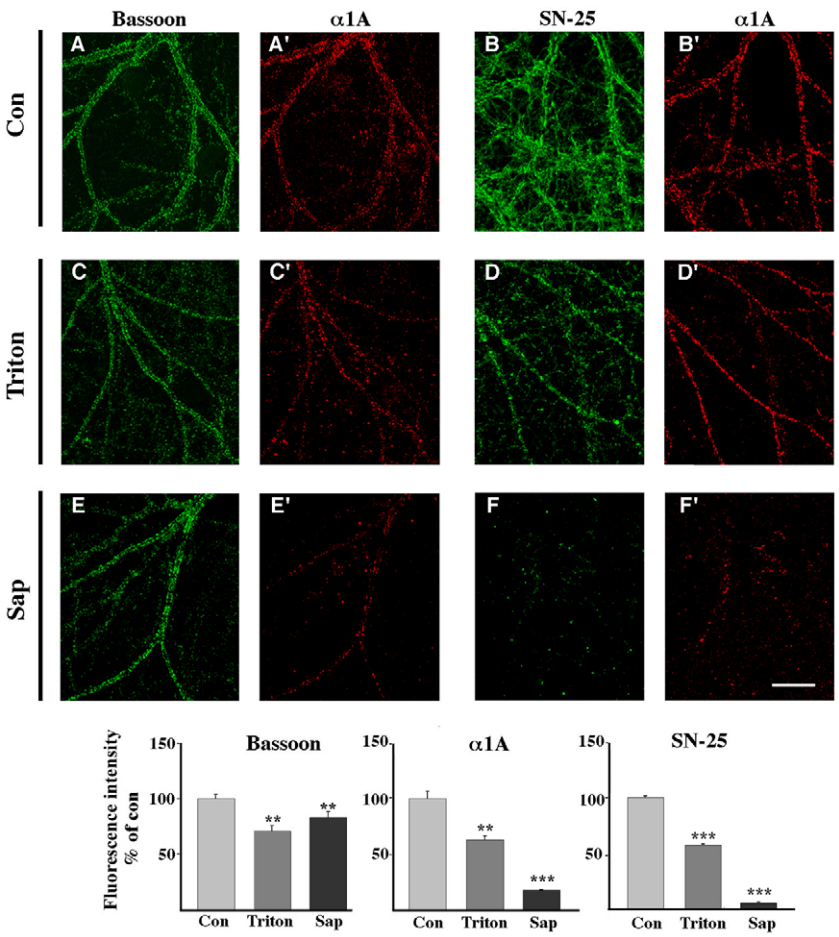

Fig. 2. Clusters of α1A and SNAP-25 are Triton-resistant. Untreated 24-DIV hippocampal neurons (Con; **A**,**A′**,**B**,**B′**), or neurons treated with Triton X-100 (Triton; **C**,**C′**,**D**,**D′**), or saponin and Triton X-100 (Sap; **E**,**E′**,**F**,**F′**) were double immunolabelled for bassoon (A,C,E) and α1A (A′,C′,E′), or SNAP-25 (SN-25; B,D,F) and α1A (B′,D′,F′). Scale bar: 20 μm. After immunolabelling, the images were recorded using a confocal microscope. (Bottom) Fluorescence intensities were quantified as described in Materials and Methods, and expressed as percentages (means ± s.e.m.) of the intensity in the untreated control neurons (ten images for each condition, acquired from three independent experiments and two coverslips for experiment, were used for quantification). The level of bassoon in the Triton-treated neurons was 70.82±4.76% of that measured in the controls (***P*=0.0082), α1A 62.95±3.53% (***P*=0.0078) and SNAP-25 (SN-25) 57.16±1.35% (****P*<0.0001). In the neurons treated with saponin and Triton X-100 (Sap), the levels were respectively 83.18±4.76% (***P*<0.05), 17.83±0.42% (****P*=0.0002) and 5.27±0.55% (****P*<0.0001).

n=27 neurons from two experiments). There was almost no difference in cholesterol levels between the untreated and fumonisin-B-treated neurons (91.65±3.82% of control, *P*=0.16; *n*=21 neurons from two experiments, not shown), but there was a significant reduction in the levels of the glycolipid GM1 (to ~55%, of control *n*=2), thus indicating impaired sphingolipid synthesis (Fig. 3B) in line with previous observations (Hering et al., 2003).

We next examined whether these treatments altered cell viability and affected protein synthesis by concentrating on synaptic proteins. Propidium iodide and Hoechst double staining showed that the viability of the cells was not significantly altered by any of the treatments (data not shown). Furthermore, the inhibition of cholesterol or sphingolipid synthesis did not significantly impair protein synthesis as demonstrated by electrophoresis, western blot analysis and the quantification of synaptic proteins (Fig. 3C,D).

To assess the effects of the drugs on the DRM distribution of synaptic proteins, we evaluated the distribution of the t-SNARE syntaxin-1, and synaptotagmin-1, synaptophysin and VAMP-2 (Fig. 4). In line with the results shown in Fig. 1, a substantial amount of the flotillin in untreated neurons was found in fractions 2-4 (50% of the total protein detected in the gradient lipid microdomains was recovered in these fractions), whereas the amount of the protein detected in the lighter fractions after mevastatin or fumonisin B treatment was considerably reduced (only 15% was recovered in fractions 2-3). Consistent with these data, about 20% of syntaxin-1 and synaptophysin, and 25% of synaptotagmin-1 and VAMP-2 were recovered in the DRM fractions of untreated neurons, whereas the amount of all four proteins detected in fractions 2-4 was reduced to 12, 7, 9 and 8.6%, respectively, after mevastatin, and 14%, 8.5%, 9% and 8%, respectively, after fumonisin B. The reduction in protein in the lighter fractions was even greater after treatment with zaragozic acid as quantitative analysis showed that only 1.7, 3.6, 1.5 and 0.8% of total synaptotagmin-1, syntaxin-1, synaptophysin and VAMP-2 were recovered in fractions 2-4 (*n*=2).

Taken together, these data indicate that under our experimental conditions fumonisin B and zaragozic acid reduce the synthesis of sphingolipids and cholesterol, but leaving the synthesis of synaptic vesicle proteins largely unaffected. By contrast, zaragozic acid affects DRMs more efficiently than fumonisin B and mevastatin.

Effects of cholesterol- and sphingolipid-perturbing drugs on presynaptic boutons and synaptic vesicle ultrastructures

On the basis of the above results, we used fumonisin B and zaragozic acid to investigate the role of sphingolipids and cholesterol in synaptic vesicle exo-endocytosis. To this end, we first analysed whether the reduction in lipids modified the structure of synaptic boutons or synaptic vesicles, by means of electron microscopy. As shown in Fig. 5, there was no difference in the ultrastructure of the presynaptic terminals between the treated and untreated neurons. In particular, the diameter of the synaptic vesicles was unchanged (control, 33.85±0.84 nm, *n*=863; fumonisin B, 37.49±0.40 nm, *n*=920; zaragozic acid, 35.08±0.89 nm, *n*=1072), and the number of vesicles per bouton was similar (control, 73.5±12.57, *n*=12; fumonisin B, 114.4±10.80, *n*=8; zaragozic acid, 82.46±12.18, *n*=12).

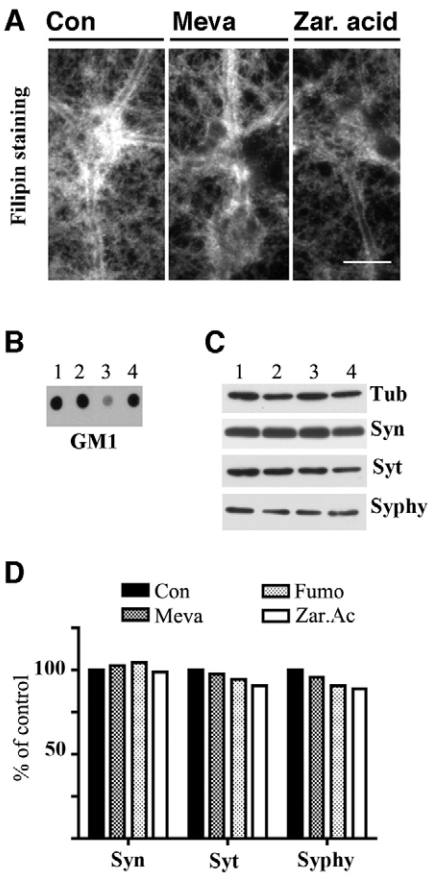

Fig. 3. Effects of drugs on cholesterol, sphingolipid and protein levels. (**A**) 14-DIV hippocampal neurons were left untreated (Con) or incubated with mevastatin (Meva) or zaragozic acid (Zar.acid) for 7 days. They were then fixed, labelled with filipin, and analysed as described in Materials and Methods. Scale bar: 10 µm. (**B**) Cell extracts (2 µl) from the control (lane 1) and from neurons treated with mevastatin (2), fumonisin B (3) or zaragozic acid (4) were spotted on NC filters and stained for GM1 using peroxidase-conjugated cholera toxin. (**C**) Equal volumes (30 µl) of cell extracts from the control (1) and from neurons treated with mevastatin (2), fumonisin (3) and zaragozic acid (4) were analysed by SDS-PAGE. The proteins were transferred to NC filters and immunolabelled for tubulin (Tub), syntaxin-1 (Syn), synaptotagmin-1 (Syt) or synaptophysin (Syphy). (**D**) Quantitative analysis of the autoradiograms. The data are expressed as percentages of untreated neurons (Con) and represent the mean values of two independent experiments.

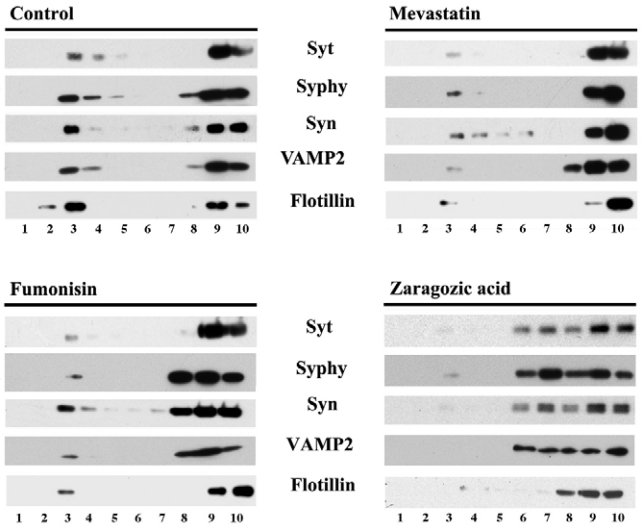

Fig. 4. Effects of cholesterol and sphingolipid depletion on lipid microdomains. Untreated neuronal cultures (Control), and cultures treated with mevastatin and mevalonate (Mevastatin), fumonisin B or zaragozic acid were lysed in 1% (w/v) Triton X-100 at 4°C, and loaded at the bottom of continuous sucrose capillary gradients. Aliquots of the gradient fractions (lanes 1-10) were analysed for the distribution of synaptotagmin-1 (Syt), synaptophysin (Syphy), syntaxin-1 (Syn), VAMP2 and flotillin by means of western blotting.

Zaragozic acid affects FM1-3 uptake

In order to analyse whether sphingolipid and/or cholesterol depletion modifies synaptic vesicle exo- and endocytosis, we incubated hippocampal neurons during depolarisation with the fluorescent styryl dye FM1-43, which reversibly binds membranes and is specifically taken up into synaptic vesicles in an activity-dependent manner during vesicle recycling (Betz and Bewick, 1992). Untreated neurons, or neurons treated with fumonisin B, mevastatin, mevalonate or zaragozic acid for 7 days, were incubated for 1 minute in the presence of FM1-43FIX diluted in depolarising (55 mM KCl) or control Krebs-Ringer-HEPES (KRH) buffer (5 mM KCl). Upon depolarisation, the control cultures showed a large number of dot-like structures loaded with the dye (Fig. 6 and supplementary material Fig. S3, Con) distributed along the dendritic branches (as demonstrated by immunolabelling with MAP-2), and largely colocalised with the synaptic marker VAMP-2 (supplementary material Fig. S3). The specificity of FM1-43FX uptake was tested by incubating the culture with 5 mM KCl-containing buffer or Ca^{+2}-deprived depolarising buffer: no significant labelling of synaptic terminals was observed under either conditions (data not shown).

Neurons treated with fumonisin B, mevastatin or zaragozic acid and incubated with the styryl dye in high-KCl buffer showed dot-like structures along the dendrites colocalising with VAMP-2 (supplementary material Fig. S3), but the uptake of FM1-43 into synaptic terminals was significantly reduced after zaragozic acid treatment (see Fig. 6 and supplementary material Fig. S3). Analysis of the pixel intensities of approximately 1000 synapses for each condition (see details in figure legends) showed that the intensity of FM1-43 in the presynapses of the neurons treated with zaragozic acid was about 50% of that found in controls (55.43±6.95%), whereas no significant changes were observed in the cultures treated with fumonisin B (Fig. 6 and supplementary material Fig. S3). Interestingly, no changes in FM1-43 uptake (86%±16.64 of control) were observed with mevastatin and mevalonate, which is in line with the observation that these drugs reduce the amount of cholesterol by only 20% under our conditions (supplementary material Fig. S3).

We next investigated whether the FM1-43 puncta underwent unloading. As shown in Fig. 6, whereas incubation with depolarisation buffer effectively de-stained the loaded fluorescence in both the control and fumonisin-B-treated neurons, we observed a reduction in the unloading efficiency in the neurons treated with zaragozic acid (Fig. 6 and data not shown).

Zaragozic acid affects anti-synaptotagmin-1 IgG uptake

We next analysed the synaptic vesicle cycle using a well-characterised method based on the use of an antibody against the luminal epitope of the synaptic vesicle protein synaptotagmin-1 (Matteoli et al., 1992).

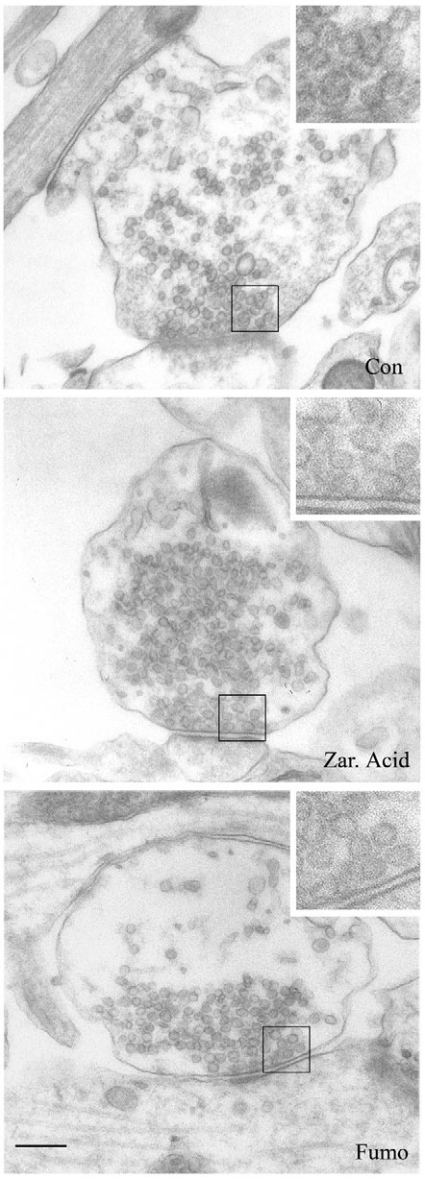

Fig. 5. Electron microscopy of synaptic boutons. Ultrathin sections of untreated hippocampal neurons (Con), and neurons incubated with zaragozic acid (Zar. Acid) or fumonisin B (Fumo). Scale bar: 200 nm. The inserts in each panel show twofold enlargements of the synapses. Note that there are no major differences in the ultrastructure, size or number of synaptic vesicles between the cholesterol- and sphingolipid-depleted neurons.

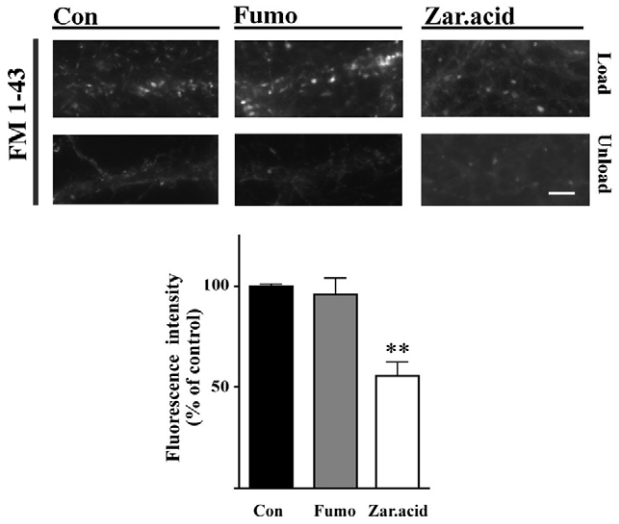

Fig. 6. FM1-43 uptake is altered after zaragozic acid treatment. Untreated hippocampal neurons (Con), or neurons incubated with fumonisin B (Fumo) or zaragozic acid (Zar. acid) were loaded with FM1-43 (Load) or, after extensive washes, incubated for 90 seconds in depolarisation buffer (Unload). Scale bar: 5 µm. The intensity of the FM1-43-labelled puncta (about 1000-1200 puncta for each condition) was measured in images (control, 10; fumonisinB and zaragozic acid, 12) taken under identical condition from three independent experiments and the data are expressed as percentages of the control (means ± s.e.m.). FM1-43 intensity was 96.03±7.83% after incubation with fumonisin B and 55.43±6.95% (**P=0.0030) after incubation with zaragozic acid. Equal areas of the FM1-43-positive puncta were measured in the control, fumonisin-B- and zaragozic-acid-treated neurons

Hippocampal neurons from untreated cultures or cultures treated with zaragozic acid or fumonisin B were incubated in a depolarising medium containing anti-synaptotagmin-1 antibodies, and then washed to allow the recycling of the synaptic vesicle membranes and consequent internalisation of the antibody. After formaldehyde fixation and permeabilisation, the anti-synaptotagmin-1 antibodies were revealed by means of immunolabelling with rhodamine-conjugated anti-IgG, whereas the pool of synaptic vesicles was immunolabelled with an antibody against VAMP-2. Both the control and drug-treated neurons showed puncta immunoreactive for VAMP-2 and anti-synaptotagmin-1 IgG (supplementary material Fig. S4), but the intensity of the immunostaining for synaptotagmin-1 antibodies was greatly reduced in the zaragozic-acid-treated neurons. Quantitative analysis of the fluorescence intensity, acquired from approximately 1000 synaptic boutons for each condition, demonstrated that the intensity of anti-synaptotagmin-1 IgG in the pre-synapses of the neurons treated with zaragozic acid was about 60% of controls (supplementary material Fig. S5). In the light of this result we next investigated the effects of cholesterol depletion specifically on the uptake of anti-synaptotagmin antibodies in either glutamatergic or GABAergic synapses. After fixation, neurons were double labelled with antibodies directed against either the vesicular glutamate transporters 1 and 2 (v-Glut) or the vesicular γ-aminobutyric acid (GABA) transporter (v-GAT; Figs 7, 8). The analysis of confocal images, collected from different experiments, revealed that the anti-synaptotagmin-1 antibodies accumulated in glutamatergic and GABAergic synapses of control neurons and that a significant reduction in immunolabelling occurred in both types of synapses after cholesterol reduction. Quantification of the fluorescence intensity in either v-Glut or v-GAT synaptic boutons, revealed that the anti-synaptotagmin-1 antibody uptake was significantly reduced in both glutamatergic and GABAergic synapses of zaragozic-acid-treated neurons (about 52% and 70% of controls, respectively; Fig. 9). Taken together, these data suggest that zaragozic acid, but not fumonisin B, inhibits the cycling of synaptic vesicles and that the vesicles of both glutamatergic and GABAergic synapses are affected.

Anti-synaptotagmin-1 IgG uptake in zaragozic-acid-treated neurons is restored by cholesterol reloading

We next investigated whether the effects on synaptic vesicle cycling observed with zaragozic acid depended on cholesterol depletion and

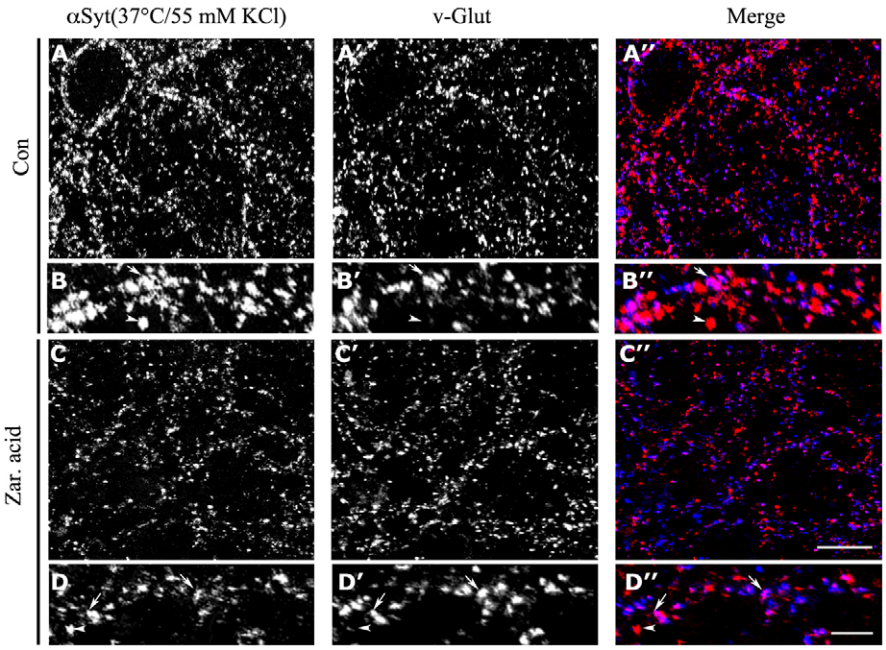

Fig. 7. Analysis of the synaptic vesicle exo-endocytic cycle in v-Glut-positive synapses. Untreated hippocampal neurons (Con; **A-B″**) or neurons treated for 7 days with zaragozic acid (**C-D″**) were incubated at 37°C in a high potassium concentration buffer containing a monoclonal antibody against the luminal domain of synaptotagmin-1 (αSyt; 37°C, 55 mM KCl). After being fixed and permeabilised, the neurons were incubated with rhodamine-conjugated anti-mouse IgG (A-D) and polyclonal antibodies directed against v-Glut1 and 2 (v-Glut) revealed by Cy5-conjugated anti-rabbit IgG (A′, B′,C′,D′); merged images are shown in A″,B″,C″,D″. In B-B″ and D-D″ arrows indicate v-Glut-positive synapses; arrowheads v-Glut-negative synapses. Scale bars: 10 μm (A-A″ and C-C″); 5 μm (B-B″ and D-D″).

not a toxic side effect of the drug. To this end, treated neurons were incubated for 30 minutes at 37°C with cholesterol-loaded MBCD (MBCD:cholesterol) (Taverna et al., 2004). After incubation with MBCD:cholesterol, the cholestrol in zaragozic-acid-treated neurons increased until it was similar to that observed in control neurons, as assessed by filipin staining and the quantitative analyses of fluorescence images from two independent experiments (Fig. 10A). After cholesterol reloading, the effects of zaragozic acid were largely reversed and the uptake of anti-synaptotagmin IgG into synaptic vesicles was almost similar to that observed in the control neurons as revealed by the quantitative analysis of neurons incubated with anti-synaptotagmin-1 IgG during depolarisation as described above (Fig. 10B).

Reduction of anti-synaptotagmin-1 IgG uptake in cholesterol depleted neurons is not dependent on calcium channel activity

Previous data have shown that $Ca_v2.1$ calcium channels, which play a major role in synaptic vesicle exocytosis, are also localised in lipid microdomains, where they colocalise and interact with SNARE proteins (Taverna et al., 2004; Taverna et al., 2007). As disruption of the lipid microdomains with MBCD causes the dissociation of $Ca_v2.1$-SNARE complexes and inactivates the channel, we investigated whether the effects observed after cholesterol depletion were solely due to channel inactivation, by incubating neurons in hypertonic sucrose (see Materials and Methods), a condition that is known to trigger exocytosis in a manner that does not require

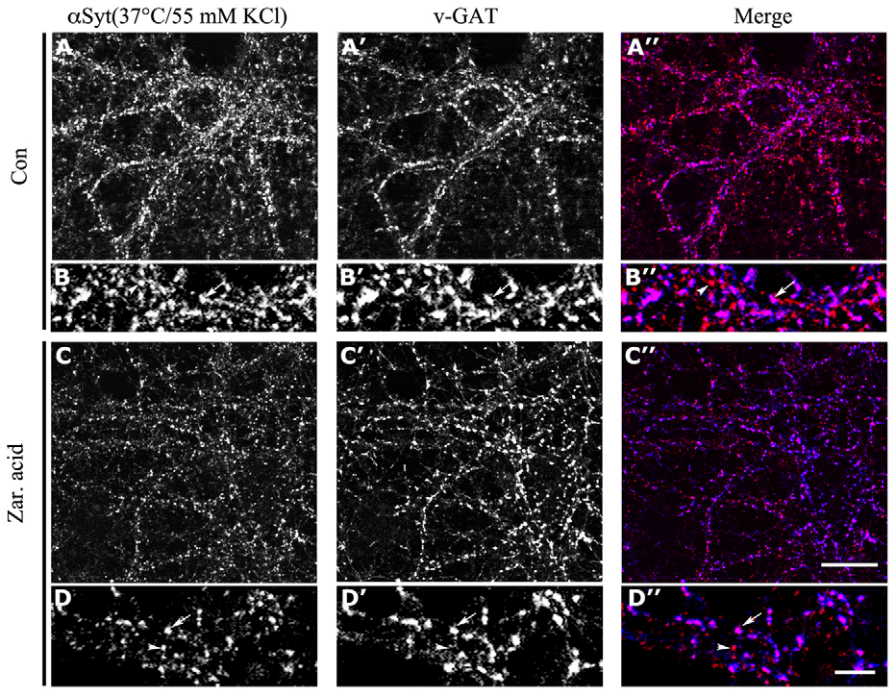

Fig. 8. Analysis of the synaptic vesicle exo-endocytic cycle in v-GAT-positive synapses. Untreated hippocampal neurons (Con; **A-B″**) or neurons treated for 7 days with zaragozic acid (**C-D″**) were incubated at 37°C in a high potassium concentration buffer containing a polyclonal antibody against the luminal domain of synaptotagmin-1 (αSyt; 37°C, 55 mM KCl). After being fixed and permeabilised, the neurons were incubated with rhodamine-conjugated anti-rabbit IgG (A-D) and antibodies directed against v-GAT revealed by Cy5-conjugated anti-guinea pig IgG (A′,B′,C′,D′); merged images are shown in A″,B″,C″,D″. In B-B″ and D-D″ arrows indicate v-GAT-positive synapses,; arrowheads v-GAT-negative synapses. Scale bars: 10 μm (A-A″ and C-C″); 5 μm (B-B″ and D-D″).

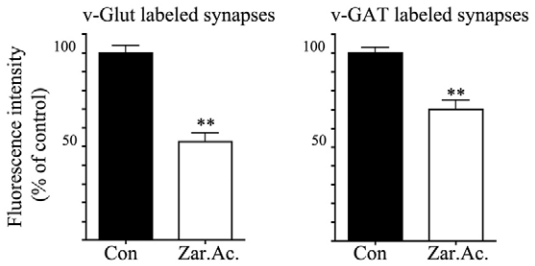

Fig. 9. Anti-synaptotagmin-1 IgG uptake is decreased in glutamatergic and GABAergic synapses of zaragozic-acid-treated neurons. The average intensity of the anti-synaptotagmin-1-immunolabelled puncta colocalising with either v-Glut1,2 (v-Glut-labelled synapses) or v-GAT was measured in control and zaragozic-acid-treated neurons and expressed as percentages of the control (means ± s.e.m.). About 850 (control) and 900 (zaragozic acid) glutamatergic synapses (from six and seven images, respectively, from three independent experiments) were analysed. For GABAergic synapses, the analysis was performed on 1050 (control) and 1150 (zaragozic acid) boutons (12 confocal images for each condition, from three independent experiments). Anti-synaptotagmin-1 fluorescence intensity after treatment with zaragozic acid (Zar.Ac.) was compared with controls, 52.61±4.50% (**P=0.0013) in the v-Glut-labelled synapses and 70.17±4.85% (**P=0.0008) in the v-GAT-labelled synapses.

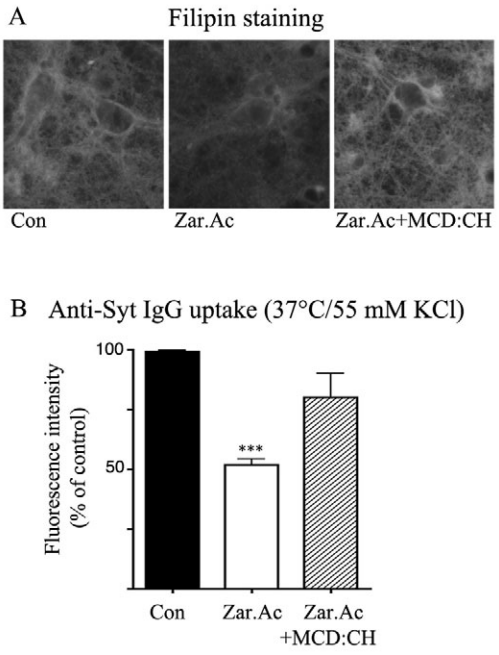

Fig. 10. Cholesterol reloading of zaragozic-acid-treated neurons restores anti-synaptotagmin-1 IgG uptake. (**A**) Untreated hippocampal neurons (Con) and neurons treated with zaragozic acid (Zar.Ac) with and without cholesterol-loaded MBCD (MCD:CH) for 30 minutes at 37°C were fixed, labelled with filipin, and analysed as described in Materials and Methods. (**B**) Living neurons as in A were washed and incubated at 37°C in a high potassium concentration buffer containing the monoclonal antibody against the luminal domain of synaptotagmin-1 (anti-Syt; 37°C, 55 mM KCl). The neurons were fixed and processed for immunofluorescence and quantitative analysis as described in supplementary material Figs S4 and S5. The intensity of anti-synaptotagmin staining in presynaptic boutons was determined from four independent experiments (about 1200 puncta and 12 images for each condition were measured) and the data are expressed as percentage of the control (Con; means ± s.e.m.). The average intensity of the anti-synaptotagmin-1 IgG-immunolabelled puncta was 51.89±2.48% of the control (***P<0.001) after incubation with zaragozic acid (Zar.Ac.) and 80.12±10.07% (P>0.01) after incubation with zaragozic acid and cholesterol-loaded MBCD (Zar.Ac+MCD:CH).

Ca^{2+} entry and therefore calcium channel activity (Rosenmund and Stevens, 1996). Untreated hippocampal neurons, or neurons treated with zaragozic acid were incubated in a high-sucrose solution containing anti-synaptotagmin-1 antibodies, and then washed, fixed and immunolabelled as described above. A number of VAMP-2- and anti-synaptotagmin-1-immunoreactive puncta were observed in the control neurons (Fig. 11); the cholesterol-depleted cells also showed synapses immunolabelled for VAMP-2 and synaptotagmin-1 IgG, but there were fewer puncta immunolabelled for synaptotagmin-1 antibodies, and the intensity measured on approximately 1000 synaptic boutons was 65% that of controls (Fig. 11).

Cholestrol reduction alters synaptic vesicle exocytosis

Previous results suggest that cholesterol plays a role in synaptic vesicle cycle, but assays based on the uptake of ligands diluted in the extracellular milieu during depolarisation are unable to identify whether cholesterol depletion was affecting exocytosis. We investigated this by means of time-lapse confocal microscopy using SypH to visualise exocytosis upon depolarisation.

Hippocampal neurons were transfected with cDNA encoding for ecliptic SypH (Miesenböck et al., 1998), and coverslips with untreated neurons or neurons treated with zaragozic acid were transferred in a perfusion chamber. Confocal images of cells maintained in standard KRH medium, buffered to pH 7.4, were recorded after perfusion with high-potassium KRH and used to quantify the increase in the fluorescence intensity of SypH after depolarisation. As shown in Fig. 12, fluorescence intensity increased above resting conditions in puncta detected in both control and zaragozic-acid-treated samples. However, after depolarisation, the mean intensity measured in 95 boutons was 4.49±0.29 times that measured under resting conditions in the controls, whereas it was 3.03±0.25 times that measured under resting conditions in the samples treated with zaragozic acid.

Discussion

The aim of this study was to investigate the role of structural lipids such as cholesterol and/or sphingolipids in presynapse physiology and, to this end, we monitored the effects of the pharmacological alteration of cholesterol or sphingolipid levels on synaptic vesicle cycling. Our results indicate that reduced cholesterol levels impair synaptic vesicle exocytosis: (1) treatment with zaragozic acid (but not fumonisin B) reduces the uptake of FM1-43 or anti-synaptotagmin-1 antibodies by synaptic boutons and, most importantly, the increase in SypH fluorescence intensity induced by the depolarisation of synaptic boutons was significantly less in cholesterol-depleted neurons; (2) the ultrastructure and number of synaptic vesicles in the synapses was not altered by treatment with either drug, suggesting that the effects observed after zaragozic acid treatment are not due to the inhibition of synaptic vesicle biogenesis; (3) the reduction in anti-synaptotagmin-1 antibody uptake induced by zaragozic acid was almost completely counteracted by cholesterol reloading; and (4) fumonisin B and zaragozic acid reduce

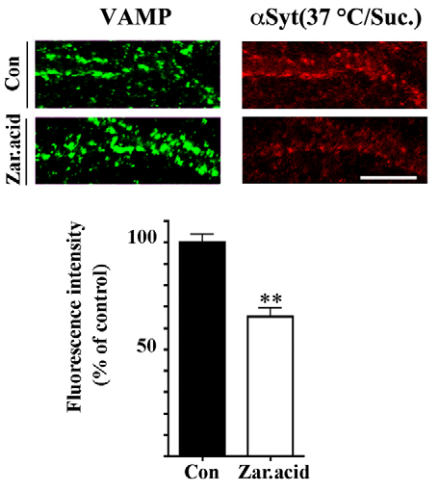

Fig. 11. Anti-synaptotagmin-1 IgG uptake upon hypertonic buffer stimulation is decreased in zaragozic-acid-treated neurons. Untreated living hippocampal neurons (Con) or neurons treated for 7 days with zaragozic acid were incubated at 37°C in hypertonic (500 µM) sucrose buffer containing a monoclonal antibody against the luminal domain of synaptotagmin-1 (anti-Syt, 37°C/Suc.). After being fixed and permeabilised, the neurons were incubated with rhodamine-conjugated anti-mouse IgG (right panels) and immunolabelled for VAMP-2. Scale bar: 10 µm. The intensity of the anti-synaptotagmin-1 immunolabelling, characterised as synaptic terminals on the basis of their colocalisation with VAMP-2 (see also supplementary material Fig. S4), was measured under both conditions (about 1000-800 puncta and ten images for each condition, from three independent experiments) and is expressed as a percentage of control (means ± s.e.m.). Anti-synaptotagmin-1 IgG fluorescence intensity after zaragozic acid (Zar.Ac) was 65.39±3.87% that of the control (**P=0.0030).

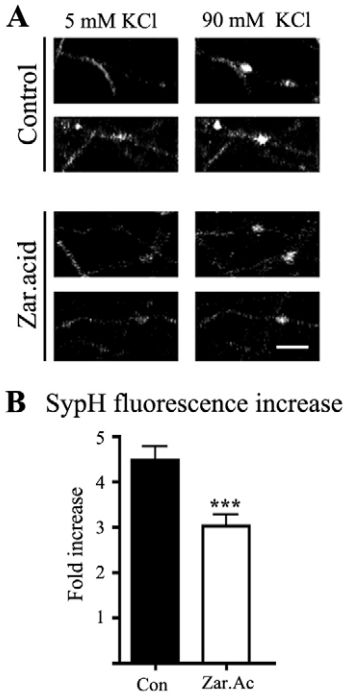

Fig. 12. In vivo imaging of SypH fluorescence upon depolarisation. (**A**) Hippocampal neurons plated onto 24-mm coverslips were transfected with cDNA encoding for ecliptic SypH and then treated with (Zar.acid) or without 5 µM zaragozic acid (Control) as described in Materials and Methods. The coverslips were mounted in a perfusion chamber on the stage of an LSM 510 Meta confocal microscope, and images were collected from neurons immediately before (5 mM KCl) and 2 minutes after perfusion with high-potassium KRH (90 mM KCl). Scale bar: 5 µm. (**B**) The fluorescence intensity of individual boutons (95 for control and 90 for zaragozic-acid-treated neurons) was measured under resting condition and after stimulation. The data are expressed as fold increase over the fluorescence intensity measured under resting conditions. Responding synapses were defined as those in which SypH intensity was 50% more than that measured at rest. Sixteen coverslips of untreated neurons (Con) and 18 of zaragozic-acid-treated neurons (Zar. Ac.), from eight independent experiments, were analysed. Data are mean ± s.e.m. ***P=0.0002).

sphingolipid and cholesterol levels, respectively, with similar efficiency, suggesting that the absence of effects on synaptic vesicles observed with fumonisin B is not due to a lack of inhibition of sphingolipid synthesis. However, analysis of synaptic function in D. melanogaster ceramidase mutants supports the involvement of sphingolipids in synaptic vesicles fusion and trafficking (Rohrbough et al., 2004). In addition, a very recent study by Darios et al. (Darios et al., 2009), suggests that endogenous sphingosine, enzymatically produced by neuron incubation with sphingomyelinase, has a stimulating effects on synaptic vesicle exocytosis. This occurs through enhancement of SNARE assembly by release of the cytosolic portion of VAMP-2 from interacting with vesicular membrane phospholipids. Based on these results, it cannot be excluded that a more significant inhibition of sphingolipid synthesis, than that obtained with a pharmacological treatment, might have stronger impact on synaptic vesicle exocytosis.

Role of cholesterol in synaptic vesicle exocytosis

Our findings show that cholesterol reduction impairs synaptic vesicle exocytosis and that the effects observed with the squalene synthase inhibitor are compatible with a real reduction in cholesterol levels and not with an effect on small GTP-binding proteins (Rab proteins), which are also important for vesicle cycling and trafficking (Fischer von Mollard et al., 1994; Jahn et al., 2003). Furthermore, the effects on the uptake of anti-synaptotagmin-1 IgG observed after drug treatment could be counteracted by treatment with cholesterol-loaded MBCD, which indicates the specific role of the lipid and not a toxic effect of the drug on neurosecretion.

The reduction in FM1-43 and anti-synaptotagmin-1 IgG uptake is more probably due to impaired vesicle cycling than to a reduction in the number or size of synaptic vesicles. This is because the ultrastructure of the nerve terminals of the cholesterol-treated hippocampal neurons was largely preserved under resting conditions, and the total number of synaptic vesicles per bouton and in the active zone was not different from that observed in control neurons, which suggests that their biogenesis was not greatly affected by cholesterol removal. These results apparently contradict those obtained in PC12 cells after acute MBCD treatment (Thiele et al., 2001), but they were obtained in neurons after a chronic decrease in cholesterol, which might slow the kinetics but not completely block the biogenesis of synaptic vesicles. Furthermore, the kinetics of synaptic vesicle biogenesis in neurons might be different from that observed in neuroendocrine cells.

As proteins of both the exocytic and endocytic machinery have been found in lipid microdomains (Salaun et al., 2004; Taverna et al., 2004; Jia et al., 2006), cholesterol might affect the fusion of synaptic vesicle membranes to the plasma membrane and/or their endocytosis. Although we cannot exclude a role of cholesterol also

in endocytosis, the analysis of SypH-transfected neurons clearly demonstrates that the exocytosis of synaptic vesicles is impaired by cholesterol reduction. This conclusion is consistent with previous data showing a large reduction of evoked synaptic transmission in MBCD-treated crayfish neuromuscular junctions and hippocampal neurons (Zamir and Charlton, 2006; Wasser et al., 2007). In addition, the removal of cholesterol was also shown to increase the spontaneous cycling of the synaptic vesicles, further suggesting that the lipid might modulate several properties of synaptic vesicle trafficking.

In line with previous observation (Salaun et al., 2004; Taverna et al., 2004; Taverna et al., 2007), it can be hypothesised that physiological levels of cholesterol are required for the function and stability of the exocytic machinery (SNARE/$Ca_v2.1$ complexes). Low membrane cholesterol levels might impair the recruitment and stability of SNARE/$Ca_v2.1$ complexes at exocytic sites or the activation of $Ca_v2.1$ channels (Tillman and Cascio, 2003; Barrantes, 2007). However, our finding that anti-synaptotagmin-1 IgG uptake is also reduced after sucrose-induced exocytosis in neurons treated with zaragozic acid seems to exclude this possibility (Rosenmund and Stevens, 1996).

The role of cholesterol in synaptic vesicles exocytosis might be because of a direct modulation of membrane properties such as membrane curvature. In this context, it is interesting to note that cholesterol plays a major role in the Ca^{2+}-triggered fusion of the cortical vesicles of sea urchin (Churchward et al., 2005; Churchward et al., 2008). Like those of cortical vesicles, synaptic vesicle membranes are particularly enriched in cholesterol (Takamori et al., 2006), and so it can be speculated that cholesterol might affect synaptic vesicles by acting directly on their membranes, for example by promoting the negative curvature important for membrane fusion. It is interesting to note that recent data have demonstrated that the addition of exogenous lysophospholipids to SNARE liposomes (which makes membrane curvature more positive) reduces the efficiency of liposome-membrane fusions (Chen et al., 2006). More recently, a link between cholesterol, membrane curvature and SNARE protein structure has been demonstrated in a cell-free assay using large unilamellar vesicles containing either t- or v-SNAREs and varying concentrations of cholesterol (Tong et al., 2009), which showed that cholesterol plays a role in modifying the v-SNARE (VAMP-2) structure in the membrane. A physiological concentration of cholesterol (40% mol of total lipids) might change the alignment of the trans-membrane domain of the v-SNARE dimers involved in SNARE complex formation from an open scissors-like shape to a parallel conformation that keeps the membrane curvature favourable for fusion. Consistent with the role of cholesterol in maintaining the correct conformation of VAMP-2, we found that a significant amount of this v-SNARE is recruited in DRMs and that zaragozic acid treatment greatly affects its distribution.

Materials and Methods

Materials and antibodies

The ultrapure Triton X-100 solution (Surfact-Amps X-100) came from Pierce (Rockford, IL), and the cholesterol, MBCD, saponin, horseradish peroxidase- and fluorescein-coupled cholera toxin subunit B, protease inhibitor cocktails, fumonisin 1, mevastatin, mevalonate, zaragozic acid and filipin from Sigma-Aldrich (Milan, Italy). The antibodies against syntaxin-1, SNAP-25, VAMP-2 (also referred to as synaptobrevin-2), MAP-2, and the anti-rabbit and mouse IgG conjugated to horseradish peroxidase came from Sigma-Aldrich; the anti-transferrin receptor from Zymed Laboratories (San Francisco, CA); the monoclonal antibodies against VAMP-2, SNAP-25, synaptotagmin-1, the rabbit polyclonal antibody against the vesicular glutamate transporter 1 and 2 and the guinea pig polyclonal antibody against the vesicular GABA transporter were from Synaptic Systems (Goettingen, Germany); the anti-bassoon antibody from Stressgen Bioreagents (Victoria, BC, Canada); and the anti-flotillin antibody from BD Biosciences (Erembodegem, Belgium). The fluorescein-, rhodamine- or Cy5-conjugated anti-mouse and rabbit IgG came from Jackson ImmunoResearch Laboratories (West Grove, PA), and the FM1-43FX from Molecular Probe (Invitrogen, San Giuliano Milanese, Italy).

Production of specific antibodies against $Ca_v2.1$

In order to analyse the distribution of the $Ca_v2.1$ channel, polyclonal antibodies against the α1A subunit (Catterall, 2000) were raised in rabbits as previously described (Taverna et al., 2007) using a synthetic peptide consisting of amino acids PSSPERAPGREGPYGRE(Cys) (see Swissprot accession no. P54282). The affinity-purified antibodies, which have previously been shown to recognise the α1A subunit by means of immunoblotting, specifically recognise the pore-forming subunit of the channel as shown by immunocytochemistry of cultured hippocampal neurons (see supplementary material Fig. S1).

Neuronal cultures, detergent and drug treatments, cholesterol re-loading

The neuronal cultures were prepared from the brains of 18-day-old rat embryos as previously described by Passafaro et al. (Passafaro et al., 2001). Briefly, the hippocampi or cortices were cut into small pieces, incubated with trypsin at 37°C, and triturated in order to obtain separated cells, which were then plated at medium-high density and grown in neurobasal medium supplemented with B27, 0.5 mM glutamine and 12.5 μM glutamate. In order to investigate protein localisation in cholesterol-dependent microdomains, cultured neurons (22 DIV) were incubated for 10 minutes on ice with 0.3% Triton X-100 or 0.3% saponin followed by 0.3% Triton X-100 as previously described (Hering et al., 2003), and were then fixed and immunostained as described above. In order to alter the endogenous level of cholesterol and sphingolipids, 14-15 DIV neurons were treated with 10 μM fumonisin B1, 4 μM mevastatin and 250 mM mevalonate, or 5 μM zaragozic acid twice, with an interval of 4 days between treatments, and then fixed or collected for Triton X-100 extraction 3 days later. To test the effects of the drugs on cholesterol synthesis, cholesterol was quantified using the Amplex Red Cholesterol Assay Kit (A12216, Molecular Probe) in accordance with the manufacturer's instructions, or after filipin staining (see below). Protein concentrations were determined using the Bio-Rad protein assay (Bio-Rad Laboratories).

For cholesterol reloading, MBCD:cholesterol complexes were prepared as described by Klein et al. (Klein et al., 1995); 15 mg of cholesterol dissolved in methanol:chloroform (2:1) were added to 10 ml of a 5% MBCD solution and incubated for 90 minutes at 80°C. Zaragozic-acid-treated neurons were reloaded with cholesterol as described (Taverna et al., 2004): briefly, neuronal cultures were incubated with 10 mM MBCD:cholesterol complex for 30 minutes at 37°C, washed carefully with pre-warmed PBS, and fixed for filipin staining or synaptotagmin-1 uptake.

SypH expression and drug treatments

Calcium-phosphate-mediated gene transfer was used to transfect the hippocampal cultures as previously described (Passafaro et al., 2003). Briefly, 6-day-old cultures plated onto 24-mm glass coverslips were incubated with 10 μg of cDNA encoding for ecliptic SypH (kindly provided by Fabio Benfenati, University of Genoa, Genoa, Italy). The cultures were treated with 5 μM zaragozic acid 6 days after transfection as described above.

Cell extracts and flotation gradients

Untreated and drug-treated neurons grown in 3 cm dishes were washed with warm PBS (37°C), scraped in 0.25 M sucrose, 4 mM HEPES-NaOH (pH 7.2), and recovered by means of centrifugation at 13,000 ***g*** for 1 hour. In order to prepare the cell extracts, the pellets were resuspended in equal volumes (400 μl) of buffer A (150 mM NaCl, 2 mM EGTA, 50 mM Tris-HCl, pH 7.5, and a Sigma-Aldrich protease inhibitor cocktail diluted 1:1000) containing 1% Triton X-100 and 1% saponin, and incubated for 30 minutes on ice. The samples were then centrifuged at 800 ***g*** for 10 minutes at 4°C, and equal volumes (30 μl) were analysed by means of SDS-PAGE and western blotting. For analysis of the lipid microdomain, the pellets were resuspended in buffer A containing 1% Triton X-100 (200-400 μg protein/50 μl). In some experiments, cholesterol was removed from the membranes before Triton X-100 solubilisation by means of treatment with 1% saponin, as previously described (Taverna et al., 2004). After 30 minutes extraction on ice, the samples were adjusted to a concentration of 1.2 M sucrose, placed in a centrifuge tube, overlaid with a discontinuous sucrose gradient (0.9, 0.8, 0.7 and 0.1 M sucrose), and the gradient was centrifuged at 137,000 ***g*** for 5 hours before ten fractions of 60 μl each were collected. Equal volumes of each fraction (20-30 μl) were analysed by means of SDS-PAGE and western blotting.

Western blotting and dot blots

Aliquots of the samples were analysed by SDS-PAGE on 6, 10 or 12% polyacrylamide gels, and were then blotted onto nitrocellulose (NC) membranes (Schleicher & Schuell, Dassel, Germany) and immunolabelled as previously described (Taverna et al., 2004; Taverna et al., 2007). In order to detect GM1, aliquots (0.2-1 μl) of each gradient fraction were spotted directly onto NC membranes, which were then probed with peroxidase-coupled cholera toxin subunit B as previously described (Taverna et al., 2007). For the quantitative analysis of synaptic proteins, neurons (300,000 per 35-mm dishes) cultured in the absence or presence of the lipid-perturbing drugs were solubilised in 300 μl of buffer A containing 1% Triton X-100 and 1% saponin, and

an equal volume of each sample was analysed by means of western blotting. In order to quantify GM1, 2 µl of each cell extract were spotted onto NC membranes and incubated with peroxidase-coupled cholera toxin subunit B. Unsaturated autoradiograms were acquired using an ARCUS II scanner (Agfa-Gevaert, Mortsel, Germany), and the density of each band or dot was quantified using NIH ImageJ software (National Technical Information Service, Springfield, VA).

Immunofluorescence

Hippocampal neurons were fixed for 8-10 minutes at room temperature with 4% paraformaldehyde in phosphate buffer, pH 7.3, containing 4% sucrose and, when required, permeabilised for 5 minutes at room temperature in PBS containing 0.3% Triton X-100. After immunostaining, as previously described (Rowe et al., 2001; Taverna et al., 2007), the images were recorded using an MRC-1024 laser scanning microscope (Bio-Rad) equipped with a 60× objective. In order to compare the double-stained patterns, the images of the fluorescein, rhodamine or Cy5 channels were acquired separately from the same areas, and superimposed. Alternatively, immunolabelled neurons were analysed using a Zeiss Axiovert 200 fluorescence microscope with a digital CCD-camera Micromax 51BFT (Crisel Instruments, Rome, Italy). The images were processed using Photoshop (Adobe Systems, Mountain View, CA). For filipin staining, after fixation with 4% paraformaldehyde, the neurons were washed with PBS, incubated for 30 minutes in 0.2 M glycine, pH 7.2, and then incubated for 1 hour with 125 µg/ml of filipin in PBS as previously described (Simons et al., 1998). The images were recorded using a Zeiss Axioplan microscope with a UV filter system (380 nm excitation, 430 nm long-pass filter), a 40× Neofluar objective, and a digital camera.

FM1-43 and anti-synapotagmin1 antibody uptake

FM1-43

Untreated hippocampal neurons, or neurons treated with lipid microdomain-depleting drugs, were incubated for 1 minute at room temperature with 3 µM FM1-43FX in normal Krebs-Ringer-HEPES (KRH; 5 mM KCl, 140 mM NaCl, 10 mM HEPES, pH 7.4, 10 mM glucose, 2.6 mM $CaCl_2$ and 1.3 mM $MgCl_2$) or high-potassium KRH buffer (55 mM KCl, 85 mM NaCl, 10 mM HEPES, pH 7.4, 10 mM glucose, 2.6 mM $CaCl_2$ and 1.3 mM $MgCl_2$) followed by three washes of 5 minutes each in Tyrode buffer (145 mM NaCl, 3 mM KCl, 10 mM HEPES, pH 7.4, 10 mM glucose, 5 µM glycine, 2.6 mM $CaCl_2$ and 1.3 mM $MgCl_2$) in the presence of 1 µM tetrodotoxin. For unloading, the neurons were further stimulated with high-potassium buffer for 2 minutes at room temperature followed by three washes with tyrode buffer in the presence of 1 µM tetrodotoxin. The neurons were fixed and immunolabelled with anti-VAMP-2 and/or anti-MAP-2 antibodies.

Anti-synaptotagmin-1 antibodies

The hippocampal neurons were incubated for 4 minutes at room temperature with a monoclonal antibody against the luminal domain of synaptotagmin-1 (Matteoli et al., 1992) in normal or high-potassium KRH buffer in the presence of $CaCl_2$ (2 mM) or EGTA (10 mM). After three washes of about 5 minutes each with normal KRH in the presence of $CaCl_2$ or EGTA and 1 µM tetrodotoxin, the neurons were fixed and incubated with a polyclonal antibody against VAMP-2. For hypertonic stimulation, the neurons were incubated in normal KRH buffer containing 500 µM sucrose for 2 minutes and processed as described above. The images were recorded using an MRC-1024 laser scanning microscope (Bio-Rad) or Zeiss LSM 510 Meta Confocal microscope with a 60× objective.

Image analyses and quantification

Detergent-treated neurons and filipin staining

The images of the control and detergent-treated neurons were recorded using identical parameters, and fluorescence intensity was determined by measuring the average pixel intensity of selected areas of soma and dendrites from ten images for each condition, acquired from three independent experiments (two coverslips per experiment). The analysis was made using NIH ImageJ software. Similarly, filipin was quantified from video images (Zeiss) of the control and of neurons treated with mevastatin and mevalonate or with zaragozic acid, recorded using identical parameters. Fluorescence intensity was determined on images collected from two experiments (two coverslips for each condition per experiment).

Synaptotagmin-1-IgG and FM1-43 uptake

In order to quantify the uptake of synaptotagmin-1 antibodies, the fluorescence intensity of labelled presynapses (identified by double-staining with anti-mouse IgG and anti-VAMP-2 rabbit antibody) was quantified using NIH ImageJ software. The images were recorded using identical parameters, and fluorescence intensity was determined by measuring the average pixel intensity of equal areas of the control or drug-treated cultures. At least three independent experiments were analysed for each condition. FM1-43-positive puncta were identified as discrete regions whose fluorescence intensity was more than twice that of the background, and the intensity of each puncta was quantified as above. Three independent experiments were analysed for each condition. In all cases, the data were expressed as percentages of control.

Electron microscopy

Hippocampal neurons were fixed on coverslips with 1.2% glutaraldehyde in 66 mM sodium cacodylate buffer, pH 7.4, post-fixed in 1% OsO_4, 1.5% $K_4Fe(CN)_6$, 0.1 M sodium cacodylate, stained with 0.5% uranyl magnesium acetate, dehydrated, and flat-embedded in Epon 812. Ultra-thin sections were observed through a Philips CM10 microscope, and the images were recorded at 28,500× magnification. The images recorded in two independent experiments were morphometrically analysed using NIH ImageJ software.

Live imaging of SypH fluorescence

Glass coverslips were mounted in a laminar-flow perfusion chamber (400 µl volume; Okolab, Ottaviano, Naples, Italy) adjusted on the stage of a LSM 510 Meta confocal microscope (Carl Zeiss) equipped with an incubator and set at 24°C. The cells were initially maintained in a standard KRH medium, buffered to pH 7.4 (see above). For depolarisation, the chamber was perfused at a rate of about 2 ml/min with a high-potassium KRH buffer (90 mM KCl, 40 mM NaCl, 10 mM HEPES, pH 7.4, 10 mM glucose, 2.6 mM $CaCl_2$, and 1.3 mM $MgCl_2$). Laser-scanning fluorescence images were acquired simultaneously using a 60× Plan Apochromat lens (1.4 NA) and pinhole set at 1.6 µm. The specimens were illuminated with 500 µW of the 488 nm line of an argon ion laser that was rapidly shuttered during all non data-acquiring periods. The fluorescence intensity of SypH during depolarisation was determined by means of time-lapse imaging using 1-minute intervals and an exposure time of 1.97 seconds. For the quantitative analyses of the increase in SypH fluorescence intensity, we used images collected immediately before and 2 minutes after the perfusion of 1 ml of high-potassium KRH medium. The quantitative measurements of fluorescence intensity at individual boutons were obtained after hand-selecting the individual regions under resting and stimulated conditions, and the changes in response to depolarisation were calculated by subtracting the initial fluorescence intensity (obtained from the pre-depolarisation fluorescence) from the fluorescence measured 2 minutes after depolarisation; the data were expressed as fold increases over pre-depolarisation fluorescence ± s.e.m.

We would like to thank Fabio Benfenati (University of Genoa, Italy) for the kind gift of cDNA encoding ecliptic SypH and Carlotta Grumelli (University of Milan, Italy) for help with anti-synaptotagmin-1 antibody uptake experiment. This study was supported by grants from the Italian Consiglio Nazionale delle Ricerche, the Ministero Istruzione Università e Ricerca (MIUR), Fondazione Cariplo (2004.1600 and 2006.0082/109251 to M.M., M.P. and P.R.); the Compagnia di San Paolo (2005.1964 to M.M., M.P. and P.R.); Progetto di ricerca ex art.56-Bando 2005, PS-NEURO/56/2005/17, EU-Synapse Integrated Project (LSHM-CT-2005-019055) to M.M. Special thanks to the Monzino Foundation (Milano, Italy) for its generous gift of the LSM 510 Meta confocal microscope.

Supplementary material available online at
http://jcs.biologists.org/cgi/content/full/123/4/595/DC1

References

Allen, J. A., Halverson-Tamboli, R. A. and Rasenick, M. M. (2007). Lipid raft microdomains and neurotransmitter signalling. *Nat. Rev. Neurosci.* **8**, 128-140.

Barrantes, F. J. (2007). Cholesterol effects on nicotinic acetylcholine receptor. *J. Neurochem.* **103**, 72-80.

Bergstrom, J. D., Kurtz, M. M., Rew, D. J., Amend, A. M., Karkas, J. D., Bostedor, R. G., Bansal, V. S., Dufresne, C., Van Middlesworth, F. L., Hensens, O. D. et al. (1993). Zaragozic acids: a family of fungal metabolites that are picomolar competitive inhibitors of squalene synthase. *Proc. Natl. Acad. Sci. USA* **90**, 80-84.

Betz, W. J. and Bewick, G. S. (1992). Optical analysis of synaptic vesicle recycling at the frog neuromuscular junction. *Science* **255**, 200-203.

Brown, D. A. and London, E. (1998). Functions of lipid rafts in biological membranes. *Annu. Rev. Cell. Dev. Biol.* **14**, 111-136.

Catterall, W. A. (2000). Structure and regulation of voltage-gated Ca^{2+} channels. *Annu. Rev. Cell Dev. Biol.* **16**, 521-555.

Chamberlain, L. H., Burgoyne, R. D. and Gould, G. W. (2001). SNARE proteins are highly enriched in lipid rafts in PC12 cells: implications for the spatial control of exocytosis. *Proc. Natl. Acad. Sci. USA* **98**, 5619-5624.

Chen, X., Araç, D., Wang, T. M., Gilpin, C. J., Zimmerberg, J. and Rizo, J. (2006). SNARE-mediated lipid mixing depends on the physical state of the vesicles. *Biophys. J.* **90**, 2062-2074.

Churchward, M. A., Rogasevskaia, T., Hofgen, J., Bau, J. and Coorssen, J. R. (2005). Cholesterol facilitates the native mechanism of Ca^{2+}-triggered membrane fusion. *J. Cell Sci.* **118**, 4833-4848.

Churchward, M. A., Rogasevskaia, T., Brandman, D. M., Khosravani, H., Nava, P., Atkinson, J. K. and Coorssen, J. R. (2008). Specific lipids supply critical negative spontaneous curvature – an essential component of native Ca^{2+}-triggered membrane fusion. *Biophys. J.* **94**, 3976-3986.

Darios, F., Wasser, C., Shakirzyanova, A., Giniatullin, A., Goodman, K., Munoz-Bravo, J. L., Raingo, J., Jorgacevski, J., Kreft, M., Zorec, R. et al. (2009). Sphingosine

facilitates SNARE complex assembly and activates synaptic vesicle exocytosis. *Neuron* **62**, 683-694.
Fischer von Mollard, G., Stahl, B., Li, C., Südhof, T. C. and Jahn, R. (1994). Rab proteins in regulated exocytosis. *Trends Biochem. Sci.* **19**, 164-168.
Garner, C. C., Kindler, S. and Gundelfinger, E. D. (2000). Molecular determinants of presynaptic active zones. *Curr. Opin. Neurobiol.* **10**, 321-327.
Golub, T. and Caroni, P. (2005). PI(4,5)P_2-dependent microdomain assemblies capture microtubules to promote and control leading edge motility. *J. Cell Biol.* **169**, 151-165.
Jahn, R., Lang, T. and Sudhof, T. C. (2003). Membrane fusion. *Cell* **112**, 519-533.
Jia, J. Y., Lamer, S., Schümann, M., Schmidt, M. R., Krause, E. and Haucke, V. (2006). Quantitative proteomics analysis of detergent-resistant membranes from chemical synapses: evidence for cholesterol as spatial organizer of synaptic vesicle cycling. *Mol. Cell Proteomics* **5**, 2060-2071.
Hering, H., Lin, C. C. and Sheng, M. (2003). Lipid rafts in the maintenance of synapses, dendritic spines, and surface AMPA receptor stability. *J Neurosci.* **23**, 3262-3271.
Kamiguchi, H. (2006). The region-specific activities of lipid rafts during axon growth and guidance. *J. Neurochem.* **98**, 330-335.
Klein, U., Gimpl, G. and Fahrenholz, F. (1995). Alteration of the myometrial plasma membrane cholesterol content with beta-cyclodextrin modulates the binding affinity of the oxytocin receptor. *Biochemistry* **34**, 13784-13793.
Lang, T., Bruns, D., Wenzel, D., Riedel, D., Holroyd, P., Thiele, C. and Jahn, R. (2001). SNAREs are concentrated in cholesterol-dependent clusters that define docking and fusion sites for exocytosis. *EMBO J.* **20**, 2202-2213.
Ledesma, M. D., Simons, K. and Dotti, C. G. (1998). Neuronal polarity: essential role of protein-lipid complexes in axonal sorting. *Proc. Natl. Acad. Sci. USA* **95**, 3966-3971.
Matteoli, M., Takei, K., Perin, M. S., Südhof, T. C. and De Camilli, P. (1992). Exo-endocytotic recycling of synaptic vesicles in developing processes of cultured hippocampal neurons. *J. Cell Biol.* **117**, 849-861.
Matteoli, M., Coco, S., Schenk, U. and Verderio, C. (2004). Vesicle turnover in developing neurons: how to build a presynaptic terminal. *Trends Cell Biol.* **14**, 133-140.
Miesenböck, G., De Angelis, D. A. and Rothman, J. E. (1998). Visualizing secretion and synaptic transmission with pH-sensitive green fluorescent proteins. *Nature* **394**, 192-195.
Mishra, S. and Joshi, P. G. (2007). Lipid raft heterogeneity: an enigma. *J. Neurochem.* **103**, 135-142.
Newey, S. E., Velamoor, V., Govek, E. E. and Van Aelst, L. (2005). Rho GTPases, dendritic structure, and mental retardation. *J. Neurobiol.* **64**, 58-74.
Passafaro, M., Piëch, V. and Sheng, M. (2001). Subunit-specific temporal and spatial patterns of AMPA receptor exocytosis in hippocampal neurons. *Nat. Neurosci.* **4**, 917-926.
Passafaro, M., Nakagawa, T., Sala, C. and Sheng, M. (2003). Induction of dendritic spines by an extracellular domain of AMPA receptor subunit GluR2. *Nature* **424**, 677-681.
Pechlivanis, M. and Kuhlmann, J. (2006). Hydrophobic modifications of Ras proteins by isoprenoid groups and fatty acids – more than just membrane anchoring. *Biochim. Biophys. Acta* **1764**, 1914-1931.
Pike, L. J. (2004). Lipid rafts: heterogeneity on the high seas. *Biochem. J.* **378**, 281-292.
Pike, L. J. (2006). Rafts defined: a report on the Keystone symposium on lipid rafts and cell function. *J. Lipid Res.* **47**, 1597-1598.
Repko, E. M. and Maltese, W. A. (1989). Post-translational isoprenylation of cellular proteins is altered in response to mevalonate availability. *J. Biol. Chem.* **264**, 9945-9952.
Rohrbough, J., Rushton, E., Palanker, L., Woodruff, E., Matthies, H. J., Acharya, U., Acharya, J. K. and Broadie, K. (2004). Ceramidase regulates synaptic vesicle exocytosis and trafficking. *J. Neurosci.* **24**, 7789-7803.
Rosenmund, C. and Stevens, C. F. (1996). Definition of the readily releasable pool of vesicles at hippocampal synapses. *Neuron* **16**, 1197-1207.
Rowe, J., Calegari, F., Taverna, E., Longhi, R. and Rosa, P. (2001). Syntaxin 1A is delivered to the apical and basolateral domains of epithelial cells: the role of munc-18 proteins. *J. Cell Sci.* **114**, 3323-3332.
Salaun, C., James, D. J. and Chamberlain, L. H. (2004). Lipid rafts and the regulation of exocytosis. *Traffic* **5**, 255-264.
Schulz, J. G., Bösel, J., Stoeckel, M., Megow, D., Dirnagl, U. and Endres, M. (2004). HMG-CoA reductase inhibition causes neurite loss by interfering with geranylgeranylpyrophosphate synthesis. *J. Neurochem.* **89**, 24-32.
Siksou, L., Rostaing, P., Lechaire, J. P., Boudier, T., Ohtsuka, T., Fejtová, A., Kao, H. T., Greengard, P., Gundelfinger, E. D., Triller, A. et al. (2007). Three-dimensional architecture of presynaptic terminal cytomatrix. *J. Neurosci.* **27**, 6868-6877.
Simons, K. and Ikonen, E. (1997). Functional rafts in cell membranes. *Nature* **387**, 569-572.
Simons, K. and Vaz, W. L. (2004). Model systems, lipid rafts, and cell membranes. *Annu. Rev. Biophys. Biomol. Struct.* **33**, 269-295.
Simons, M., Keller, P., De Strooper, B., Beyreuther, K., Dotti, C. G. and Simons, K. (1998). Cholesterol depletion inhibits the generation of beta-amyloid in hippocampal neurons. *Proc. Natl. Acad. Sci. USA* **95**, 6460-6464.
Takamori, S., Holt, M., Stenius, K., Lemke, E. A., Grønborg, M., Riedel, D., Urlaub, H., Schenck, S., Brügger, B., Ringler, P. et al. (2006). Molecular anatomy of a trafficking organelle. *Cell* **17**, 831-846.
Taverna, E., Saba, E., Rowe, J., Francolini, M., Clementi, F. and Rosa, P. (2004). Role of lipid microdomains in P/Q-type calcium channel ($Ca_v2.1$) clustering and function in presynaptic membranes. *J. Biol. Chem.* **279**, 5127-5134.
Taverna, E., Saba, E., Linetti, A., Longhi, R., Jeromin, A., Righi, M., Clementi, F. and Rosa, P. (2007). Localization of synaptic proteins involved in neurosecretion in different membrane microdomains. *J. Neurochem.* **100**, 664-677.
Thiele, C., Hannah, M. J., Fahrenholz, F. and Huttner, W. B. (2000). Cholesterol binds to synaptophysin and is required for biogenesis of synaptic vesicles. *Nat. Cell Biol.* **2**, 42-49.
Tillman, T. S. and Cascio, M. (2003). Effects of membrane lipids on ion channel structure and function. *Cell. Biochem. Biophys.* **38**, 161-190.
Tong, J., Borbat, P. P., Freed, J. H. and Shin, Y. K. (2009). A scissors mechanism for stimulation of SNARE-mediated lipid mixing by cholesterol. *Proc. Natl. Acad. Sci. USA* **106**, 5141-5146.
Tsui-Pierchala, B. A., Encinas, M., Milbrandt, J. and Johnson, E. M. (2002). Lipid rafts in neuronal signaling and function. *Trends Neurosci.* **25**, 412-417.
Wasser, C. R., Ertunc, M., Liu, X. and Kavalali, E. T. (2007). Cholesterol-dependent balance between evoked and spontaneous synaptic vesicle recycling. *J. Physiol.* **579**, 413-429.
Willmann, R., Pun, S., Stallmach, L., Sadasivam, G., Santos, A. F., Caroni, P. and Fuhrer, C. (2006). Cholesterol and lipid microdomains stabilize the postsynapse at the neuromuscular junction. *EMBO J.* **25**, 4050-4060.
Zamir, O. and Charlton, M. P. (2006). Cholesterol and synaptic transmitter release at crayfish neuromuscular junctions. *J. Physiol.* **571**, 83-99.
Zidovetzki, R. and Levitan, I. (2007). Use of cyclodextrins to manipulate plasma membrane cholesterol content: evidence, misconceptions and control strategies. *Biochim. Biophys. Acta* **1768**, 1311-1324.

Journal of Cell Science